Inorganica Chimica Acta 517 (2020) 120195

Contents lists available at ScienceDirect

Inorganica Chimica Acta

journal homepage: www.elsevier.com/locate/ica

Research paper

Synthesis, structure, and hydrogen evolution studies of a heteroleptic Co (III) complex

Michael J. Celestine [a], Mark A.W. Lawrence [b], Olivier Schott [c], Vincent Picard [c], Garry S. Hanan [c], Emily M. Marquez [a], Chekeyl G. Harold [a], Cole T. Kuester [d], Blaise A. Frenzel [d], Christopher G. Hamaker [e], Sean E. Hightower [d], Colin D. McMillen [f], Alvin A. Holder [a,*]

[a] Department of Chemistry and Biochemistry, Old Dominion University, 4541 Hampton Boulevard, Norfolk, VA 23529, USA
[b] Department of Chemistry, University of the West Indies, Mona Campus, Kingston 7, Jamaica
[c] Département de Chimie, Université de Montréal, Montréal, Canada
[d] Department of Chemistry, University of North Dakota, 151 Cornell St., Stop 9024, Grand Forks, ND 58202-9024, USA
[e] Department of Chemistry, Illinois State University, Campus Box 4160, Normal, IL 61790-4160, USA
[f] Department of Chemistry, Clemson University, 379 Hunter Laboratories, Clemson, SC 29634, USA

ARTICLE INFO

Keywords:
Cobalt(III)
Hydrogen production
Electrocatalysis
Polypyridyl ligands
Photocatalysis

ABSTRACT

[Co(tpy)(phen)Cl](PF$_6$)$_2$•0.25CH$_3$CN (where tpy = 2,2′;6′,2″-terpyridine and phen = 1,10-phenanthroline) was prepared from a one pot mixture involving stoichiometric quantities of tpy and phen. The structure of [Co(tpy)(phen)Cl](PF$_6$)$_2$•0.25CH$_3$CN was confirmed by elemental analysis, high resolution mass spectroscopy (HRMS), various spectroscopic analyses, and X-ray crystallography. Density functional theory calculations were also carried out. The crystal structure of [Co(tpy)(phen)Cl](PF$_6$)$_2$•0.25CH$_3$CN, which was grown from acetonitrile, revealed a monoclinic crystal system with a *C*2/*c* space group. The cyclic voltammogram which was acquired in acetonitrile revealed reversible $Co^{III/II}$, $Co^{II/I}$, and $Co^{I/0}$ mixed with ligand-based redox couples at $E_{½}$ = +0.35, –0.81, and –1.37 V (vs Ag/AgCl), respectively. In the presence of *p*-cyanoanillinium tetrafluoroborate with acetonitrile as the solvent, [Co(tpy)(phen)Cl](PF$_6$)$_2$•0.25CH$_3$CN displayed electrocatalytic hydrogen evolution activity at a 830 mV overpotential, as evidenced by a catalytic wave which was observed in the voltammogram, and by the detection of hydrogen in the headspace of the reaction vessel of a controlled potential electrolysis experiment. Photocatalytic hydrogen evolution studies with [Co(tpy)(phen)Cl](PF$_6$)$_2$•0.25CH$_3$CN produced a turnover frequency (TOF) of 3300 mmol H_2 mol^{-1}_{CAT} min^{-1} when compared to [Co(dmgH)$_2$(py)Cl] (where dmgH = dimethylglyoximato), which had a TOF of 4500 mmol $H_2.mol^{-1}_{CAT}$ min^{-1} under the same conditions. [Co(tpy)(phen)Cl](PF$_6$)$_2$•0.25CH$_3$CN produced a turnover number (TON) of 79 when compared to 141 for [Co(dmgH)$_2$Cl(py)] in DMF in ca 3 h.

1. Introduction

The finite nature of fossil fuels, and the lasting adverse effects caused by the by-products of their combustion [1,2] has created the need for a viable yet clean alternative fuel source. Hydrogen has been, and continues to be examined as a suitable candidate [1–5]. There are many drawbacks to the storage and transportation of hydrogen, mainly due to its highly flammable nature. As such, its generation on site and on demand is desired. A convenient way to produce hydrogen through sustainable means would be the conversion of solar energy to chemical energy through the reduction of water [6–8]. Whereas water splitting is appealing, the difficulties associated with the kinetics and thermodynamics of this multi-electron process have made the reduction of protons more appealing for the hydrogen evolution reaction (HER). Some platinum catalysts capable of reducing water to hydrogen with rates that are close to thermodynamic equilibrium have been reported in the literature [9,10]. However, due to the high cost of noble metals such as Pt, Rh, Ir, etc., there is a search for catalysts based on cheaper and slightly more abundant first row transition metals, for instance, Fe, Co, and Ni [11–17].

Cobalt-containing complexes such as the cobaloximes [18,19], polypyridyl-containing cobalt(II/III) complexes [20–23], and cobalt(II)

* Corresponding author.
E-mail address: aholder@odu.edu (A.A. Holder).

https://doi.org/10.1016/j.ica.2020.120195
Received 21 September 2020; Received in revised form 3 December 2020; Accepted 7 December 2020
Available online 11 December 2020

salen complexes [10], just to list a few, have been reported as promising candidates. In 2014 Chen et al. [11] reported on the use of a cobalt(II) catalyst, [Co(tpy)(phen)Cl]Cl, when immobilized on the surface of an electrode was able to produce hydrogen with a turn over number (TON) of about 2.2×10^6 after about 50 h. Other efforts to make HER practical included the development of photocatalytic systems. These systems are typically heterometallic in nature, with one site acting as a light antenna and the other as the catalytic site [6,8,24–27]. The polypyridyl system as developed by Chen et al. [11] may also possess photocatalytic properties, as polypyridyl ligands are known to stabilize the excited state of certain metal centres.

Whether electrocatalytic or photocatalytic in nature, the formation of either + 1 or 0 oxidation state is required from the precatalyst in most cases. This is so, as these oxidation states can facilitate the oxidative addition of a proton to form the reactive $M^{III/II}$–H species as an important species in the catalytic cycle of the HER. The choice of the ligand is thus crucial, as a change in the oxidation state may be accompanied by a change in the preferred geometry around the metal centre.

In many studies involving a cobalt-based catalyst, it is common that upon production of a cobalt(I) species that the complex undergoes a geometric change through the loss of a ligand, with nitrogen-based ligands being favoured in the coordination sphere over aqua and halogen ligands [12,19,28,29].

Herein we report the crystal structure, spectroscopic, and cyclic voltammetric properties, as well as the electrocatalytic and photocatalytic hydrogen evolution studies of [Co(tpy)(phen)Cl] $(PF_6)_2$•0.25CH_3CN (which for simplicity will be referred to as [Co(tpy)(phen)Cl]$(PF_6)_2$) in non-aqueous media. These studies are geared towards establishing the potential of this species as a photocatalyst in the HER, starting from the Co(III) analogue of the species in comparison to the Co(II) species as reported by Chen et al. [11]. This study also attempts to establish the stability of the low valent states of the title complex via cyclic voltammetry, and is also as a part of a series of studies [30] aimed at correlating the effect of the ancillary ligand on the photocatalytic response of Co(III) complexes in HER.

2. Experimental

2.1. Materials and physical measurements

All chemicals and reagents were purchased from commercial sources and were used without further purification.

2.1.1. Physical measurements

^{59}Co NMR spectra were acquired on a Bruker 400 MHz spectrometer with $K_3[Co(CN)_6]$ as an external reference in either DMSO-d_6 (δ = 289 ppm [31]) or CD_3CN (δ = 293 ppm [31]) at room temperature. ^{1}H NMR spectra were acquired on a Bruker AVANCE III 400 MHz spectrometer with either DMSO-d_6 or CD_3CN as solvent. All NMR spectra were processed with the ACD/NMR Processor Academic Edition software which was available from Advanced Chemistry Development[‡].

Microanalyses (C, H, and N) were performed by Intertek Chemical and Pharmaceuticals, 291 Route 22 East, Salem Industrial Park, Building #5, Whitehouse, NJ 08888, U.S.A.

HRMS spectra were acquired via positive electrospray ionization on a Bruker 12 Tesla APEX–Qe FTICR-MS with an Apollo II ion source at the College of Sciences Major Instrument Cluster (COSMIC), Old Dominion University, Norfolk, VA 23529, U.S.A. Samples were dissolved in acetonitrile before being introduced by direct injection using a syringe pump with a flow rate of 2 μL s^{-1}. The data was processed using Bruker Daltonics Data Analysis Version 3.4.

All electrochemical experiments were carried out on a BAS Epsilon C3 under an argon atmosphere in the respective solvent at room temperature (ca 20 °C), after sparging with argon for several minutes. A standard three electrode configuration was employed consisting of a glassy carbon working electrode (3 mm diameter) and a Pt wire as auxiliary electrode. For the reference electrode, AgCl/Ag (BASi, 3.0 M NaCl) was employed, which was separated from the analytical solution by a Vicor® frit, against which ferrocene shows a reversible wave at + 0.43 V in CH_3CN. The ionic strength was maintained at 0.1 M using [^{n}Bu_4N]ClO_4, $NaClO_4$, or NaCl, where appropriate.

Spectroelectrochemical measurements were carried out at 20 °C with a thermostatted water bath/circulator (Thermo Scientific®). Absorbance data were acquired on an Agilent® 8453A diode array spectrophotometer. A Pt gauze and a Pt wire were utilised as working and auxiliary electrodes, respectively, and AgCl/Ag (BASi, 3.0 M NaCl) was utilised as a reference electrode. The ionic strength was maintained at 0.10 M as stated above. Each solution was sparged with Ar for at least two minutes in the spectroelectrochemical cuvette (1 mm path length) prior to acquisition of the data.

2.2. Synthesis and physical measurements of the cobalt(III) complex

2.2.1. Synthesis of [Co(tpy)(phen)Cl]$(PF_6)_2$•0.25CH_3CN

A mixture of 2,2′:6′,2′′-terpyridine (0.98 g, 4.2 mmol), 1,10-phenanthroline (0.76 g, 4.2 mmol), and $CoCl_2$·$6H_2O$ (1.00 g, 4.2 mmol) were stirred in ethanol (320 mL) for 3 h. Iodine (1.31 g, 5.2 mmol) in ethanol (60 mL) was added dropwise to the resulting solution with stirring. The solution was filtered; then the filtrate was collected and NH_4PF_6 (6.86 g, 42 mmol) in methanol (60 mL) was added. The resulting mixture was filtered; then the residue air dried. The crude product was then dissolved in acetonitrile; then the solution was filtered. The filtrate which contained the crude product was purified three times by chromatography with Sephadex LH-20 as the stationary phase and acetonitrile as eluent. The product was worked up. Yield = 1.17 g (34%) A single crystal of [Co(tpy)(phen)Cl]$(PF_6)_2$ was grown as an acetonitrile solvate by slow evaporation at first in acetonitrile solution; followed by the addition of acetone. Calculated for $C_{27.5}H_{19.75}N_{5.25}ClP_2F_{12}$: C 40.88, H 2.46, N 9.10, Cl 4.39%. Found C 40.85, H 2.51, N 9.17, Cl 4.21%. HRMS (positive mode, found (calc.): $[M\text{-}1PF_6]^+$ = 652.0247 (652.0247). ^{1}H NMR (400 MHz, CD_3CN, δ/ppm) 10.21 (d, J = 5.06 Hz, 1H, phen-j'), 9.30 (d, J = 8.14 Hz, 1H, phen-h'), 8.89 (d, J = 6.82 Hz, 1H, tpy-h), 8.80–8.86 (m, 2H, tpy-g), 8.67 (d, J = 8.14 Hz, 1H, phen-a'), 8.61 (dd, J = 7.92, 5.94 Hz, 1H, phen-i'), 8.48–8.57 (m, 3H, tpy-a and phen-e'), 8.29 (d, J = 9.02 Hz, 1H, phen-f'), 8.18 (t, J = 7.59 Hz, 2H, tpy-b), 7.64 (dd, J = 7.59, 5.83 Hz, 1H, phen-b'), 7.43 (d, J = 4.84 Hz, 1H, phen -c'), 7.33 (t, J = 6.38 Hz, 2H, tpy-c), 7.18 (d, J = 5.50 Hz, 2H, tpy-d). ^{1}H NMR (400 MHz, DMSO-d_6, δ/ppm) 10.12 (d, J = 5.06 Hz) 9.51 (d, J = 8.14 Hz) 9.38 (d, J = 7.92 Hz) 9.23 (m) 9.10 (m) 8.93 (m) 8.86 (d, J = 7.92 Hz) 8.75 (dd, J = 8.14, 5.50 Hz) 8.66 (d, J = 8.80 Hz) 8.43 (d, J = 8.80 Hz) 8.34 (q, J = 7.92 Hz) 7.72 (m) 7.46 (m) 7.35 (d, J = 5.50 Hz); ^{59}Co NMR (95 MHz, CD_3CN, δ/ppm) 7148; ^{59}Co NMR (95 MHz, DMSO-d_6, δ/ppm) 7177; UV–visible (CH_3CN, λ/nm (10^{-4} ε/M^{-1} cm^{-1})): 203 (78), 222 (75), 275 (39), 322 (12), and 487 (0.27).

FTIR (ATR, ν/cm^{-1}) 1606(m), 1577 (w), 1522 (m), 1483 (m), 1454 (m), 1433 (m), 769 (s), 728 (m).

2.3. Density functional theory calculations

Density functional theory calculations were carried out using the GAMESS software package[§] [32,33]. The structures were optimized in the gas phase as indicated by the absence of imaginary frequencies in the Hessian, EDF1/6-31G(d) [34–36]. The GAMESS input file was generated

[‡] ACD, Inc., 8 King Street East, Suite 107, Toronto, Ontario M5C 1B5, Canada.

[§] GAMESS: an open-source general ab initio quantum chemistry package. https://www.msg.chem.iastate.edu/gamess/index.html

using MacMolPlt 7.7** [37], and the output file viewed using the same.

2.4. X-ray crystallography

Single crystal X-ray diffraction was carried out at 150 K using a Bruker D8 Quest diffractometer with Mo Kα radiation and a Photon 100 detector. The data was collected using phi and omega scans in 0.5°oscillations. The structure was solved and refined using the Bruker SHELXTL [38] Software Package. All non-hydrogen atoms were refined anisotropically, and hydrogen atoms were placed in calculated positions using riding models. The crystal was found to be the acetonitrile solvate of the target cobalt complex. The acetonitrile solvent molecule was found to be disordered and partially occupied, having 1/2 occupancy per formula unit of the cobalt(III) complex. Details of data collection and structural solution for $[Co(tpy)(phen)Cl](PF_6)_2 \bullet 0.5C_2H_3N$ are provided in the supporting crystallographic files (CIF).

2.5. Photocatalytic measurements

Hydrogen evolution was monitored using a Perkin Elmer Clarus-580 gas chromatograph (GC) with a thermal conductivity detector, argon as carrier and eluent gas, a 7′ HayeSep N 60/80 pre-column, a 9′ molecular sieve 13 × 45/60 column and a 1 mL injection loop.

Three distinct solutions for the photosensitizer, $[Ru(bpy)_3](PF_6)_2$, for the catalyst, and lastly, for the sacrificial electron donor and acid source (HBF_4, 48% water) were prepared: the three solutions were mixed together to obtain 5 mL of sample solutions in standard 20 mL headspace vials. In DMF, the resulting molar concentrations of photocatalytic components were as follows: 1 M for triethanolamine (TEOA), 0.1 M for (HBF_4), 0.56 M for water, 0.1 mM for $[Ru(bpy)_3](PF_6)_2$, 0.01 mM for [Co(tpy)(phen)Cl]$(PF_6)_2$ or $[Co(dmgH)_2Cl(py)]$ (apparent pH = 8.9). Those vials were placed on a LED panel in a thermostatic bath set at 20 °C. They were sealed with a rubber septum pierced with two stainless steel tubes. The first tube carried an argon flow saturated with spectroscopic grade solvent vapor. The flow rate was set to 5 mL min^{-1} (adjusted with a manual flow controller (Porter, 1000) and referenced with a digital flow meter (Perkin Elmer FlowMark).

The second tube leads the flow to the GC sample loop through a 2 mL overflow protection vial, then through an 8-port stream select valve (VICCI) and finally to the GC sample loop. A microprocessor (Arduino Uno) coupled with a custom PC interface allows for timed injections. For general calibration, stock cylinders of known concentration of H_2 in nitrogen replaced the nitrogen flow (inserted at the pre-bubbler, to keep the vapor matrix consistent). The acquired data, independent of flow rate (under same pressure) were easily converted into a rate of hydrogen by using equation (1). For calibration of H_2 production, a nitrogen bottle of certified 100 ppm hydrogen was set to deliver a specific flow. H_2 production rate at a specific nitrogen flow, a syringe pump (New Era Pump) equipped with a gas-tight syringe (SGE) and a 26 s gauge needle (Hamilton) was used to bubble different rates of pure hydrogen gas into the sample, to a minimum of 0.5 μL min^{-1}. This gave a linear fit for peak area for H_2 versus the flow rates of H_2 (Eq. (1)). All experiments were carried out in duplicate to verify the reproducibility of results, and an average for the TOF and TON curves was calculated with Origin software. The error associated with the TOF and TON values was estimated to be 10% [39].

$$H_2\text{rate}\left(\mu L \overset{-1}{min}\right) = [H_2\text{standard}](\text{ppm}) \times N_2\text{flowrate}\left(L^{min-1}\right) \quad (1)$$

CCDC no. 1953060 contains the supplementary crystallographic data for $[Co(tpy)(phen)Cl](PF_6)_2 \bullet 0.5C_2H_3N$. These data can be obtained free of charge from The Cambridge Crystallographic Data Centre via www.ccdc.cam.ac.uk/data_request/cif. Supporting information containing additional spectral and voltammetric characterizations are also provided.

3. Results and discussion

3.1. Synthesis

$[Co(tpy)(phen)Cl](PF_6)_2$ was synthesized (Scheme 1) using stoichiometric quantities in one pot, and was purified three times on a Sephadex LH-20 column to ensure the separation of the main by-products $[Co(tpy)_2](PF_6)_3$ and $[Co(phen)_2(solv)](PF_6)_3$ from [Co(tpy)(phen)Cl]$(PF_6)_2$. [Co(tpy)(phen)Cl]$(PF_6)_2$ was characterized by elemental analysis, HRMS, UV–visible, ^1H and ^{59}Co NMR spectroscopies, X-ray crystallography, and cyclic voltammetry. $[Co(tpy)_2](PF_6)_3$ was identified and characterized after column chromatography via ^1H and ^{59}Co NMR spectroscopy, and with ESI MS (See supporting information Figs. S1–S4).

3.2. HRMS analysis

HRMS data were acquired for [Co(tpy)(phen)Cl]$(PF_6)_2$ in CH_3CN (Fig. S5). In the HRMS, the most intense peak is observed at m/z = 652.0247, which corresponded to the loss of one of the PF_6^- counter ions to produce $(([Co^{III}(tpy)(phen)Cl](PF_6))^+)$. The HRMS data do complement the elemental analysis data and other spectroscopic characterizations.

3.3. ^1H and ^{59}Co NMR spectroscopic studies

In an NMR spectroscopic study, ^1H and ^{59}Co NMR spectra were acquired for [Co(tpy)(phen)Cl]$(PF_6)_2$ in CD_3CN or DMSO-d_6 at ambient temperature. The ^1H NMR spectra (Fig. 1B, and Fig. S6), revealed solvent peaks and aryl resonances.

In the solvent region, the presence of acetonitrile in the isolated solid was confirmed (δ = 2.07 ppm) in DMSO-d_6. In the aromatic region of the ^1H NMR spectrum, there is a significant overlap of the resonances of the tpy and phen ligands, Fig. 1A. The assignment of these peaks was guided by ^1H-^1H the COSY NMR spectrum (Fig. S7); and coordinated tpy protons are assigned to resonances at 7.18, 7.33, 8.18, 8.54, 8.83, and 8.89 ppm. Paramagnetic ^1H NMR spectroscopic studies on [Co(tpy)(phen)Cl]$(PF_6)_2$ showed no resonance between 10 and 120 ppm which suggested the absence of the cobalt(II) species in the isolated solid (see Fig. S4). ^1H NMR spectra of polypyridyl cobalt(II) complexes generally display chemical shifts in this region [40], such as $[Co(phen)_3]^{2+}$ which have chemical shifts observed at 17, 33, 50, and 107 ppm in CD_3CN. The cobalt(II) complex that was separated from target complex had observable chemical shifts at 17, 22, 33, 34, 48, 49, and 57 ppm. It should be noted that in the ^1H NMR spectrum of [Co(tpy)(phen)Cl]$(PF_6)_2$, satellite peaks can be seen in the concentrated solutions used to acquire the spectra. These satellite peaks may be the result of ligand dissociation or trace amounts of the "free" ligand from the synthesis, which the latter is the least probable. The ratio of integrals suggests that the uncoordinated ligand is less than 3% of the mixture.

^{59}Co NMR spectroscopic data as shown in Fig. 1 showed one chemical shift at 7148 ppm in CD_3CN and at 7177 ppm in DMSO-d_6. A comparison with other Co(III) complexes such as $[Co(phen)_3](PF_6)_3$ (δ = 7000 ppm in DMSO-d_6 [41], 7080 ppm [42]) or $[Co(phen)_2(bpy)](PF_6)_3 \bullet 0.5(C_2H_5)_2O$ (δ = 6900 ppm in DMSO-d_6) [41] revealed that the chemical shift of [Co(tpy)(phen)Cl]$(PF_6)_2$ is in a similar region to other cobalt(III)-containing polypyridyl complexes, which are shown in Table S1. The ^{59}Co NMR spectroscopic chemical shift of cobalt-containing complexes is very sensitive to the type(s) of ligand(s) in the coordination sphere, as well as the oxidation state of a cobalt metal centre. The absence of other peaks in the 7000 ppm region of the ^{59}Co NMR spectrum of the isolated product proved the absence of Co(III) by-

** MacMolPlt: an open-source molecular builder and visualization tool for GAMESS. http://brettbode.github.io/wxmacmolplt/

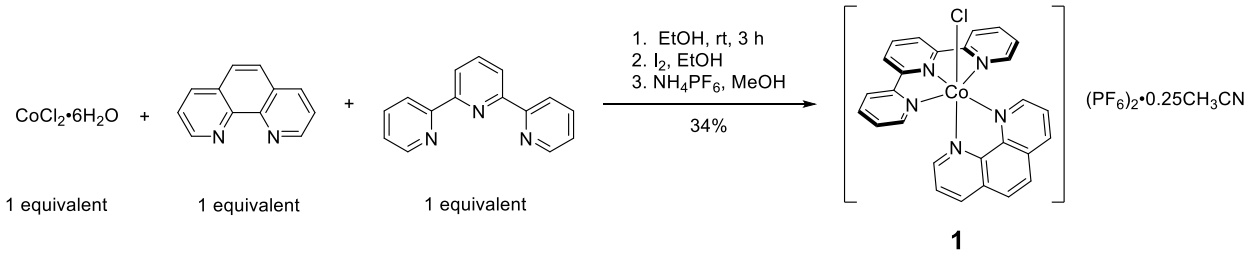

Scheme 1. Synthesis of $[Co(tpy)(phen)Cl](PF_6)_2 \bullet 0.25CH_3CN$.

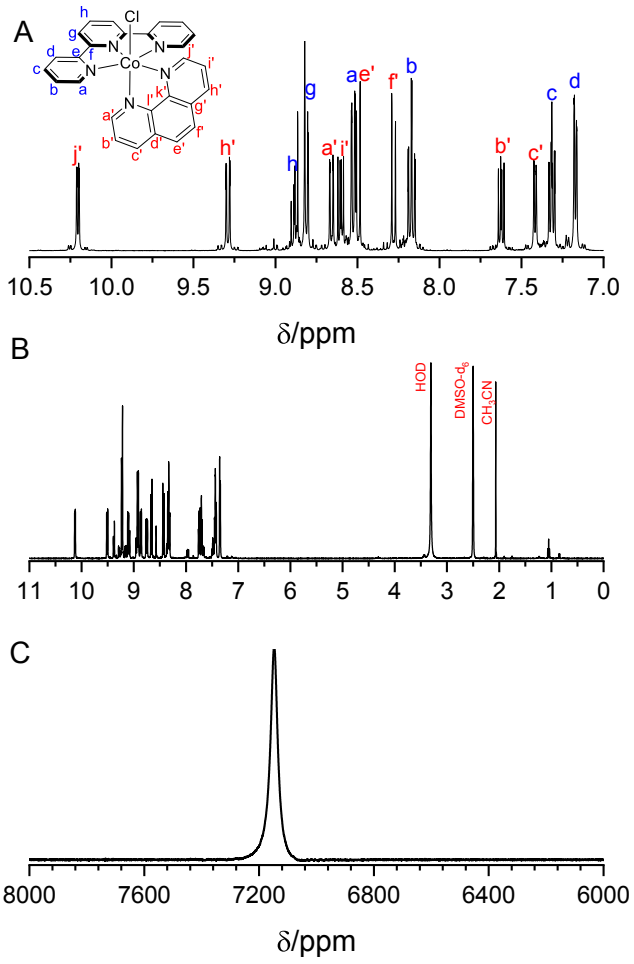

Fig. 1. ^{1}H NMR spectra of $[Co(tpy)(phen)Cl](PF_6)_2$ in CD_3CN (A) and DMSO-d_6 (B), and ^{59}Co NMR spectrum of 40 mM $[Co(tpy)(phen)Cl](PF_6)_2$ in CD_3CN (C).

products in the isolated material. It should be noted that acquisition of ^{59}Co NMR spectra of Co(II) species is very difficult and to process is also very difficult. The ^{59}Co NMR spectroscopic data (in conjunction with the ESI MS data) strongly suggest that cobalt(II) impurities and Co(III) by-products are absent from the isolated product, $[Co(tpy)(phen)Cl](PF_6)_2$.

3.4. UV–visible spectroscopic studies

The UV–visible spectrum of $[Co(tpy)(phen)Cl](PF_6)_2$ in Fig. 2 shows transitions that are consistent with d-d transitions (dual bands) at 487 nm, $\pi \rightarrow \pi^*$, intra-ligand, and metal-to-ligand charge transfer bands in the UV region. The molar extinction coefficients are 78×10^4, 75×10^4, 29×10^4, 13×10^4, and $0.27 \times 10^4\ M^{-1}\ cm^{-1}$ at 203, 222, 275, 322, and 487 nm, respectively. The dual band at 487 nm in CH_3CN is observed at

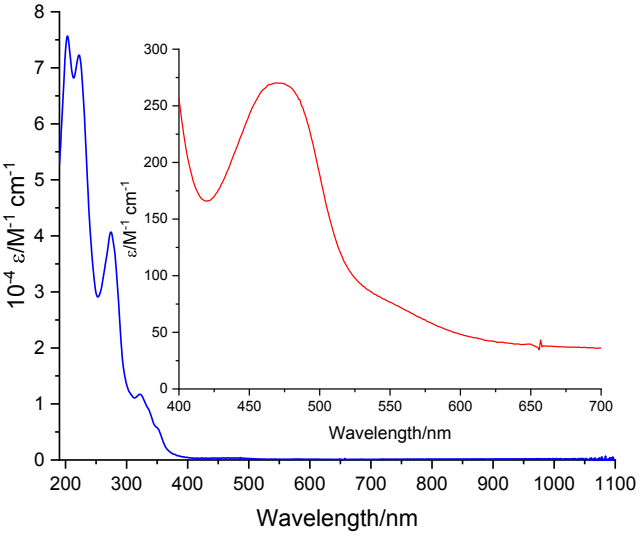

Fig. 2. UV–visible spectrum of $[Co(tpy)(phen)Cl](PF_6)_2$ in acetonitrile (400–700 nm enhanced view shown in inset).

$\lambda_{max} = 460$ nm and 491 nm, which had a hypsochromic shift in the H_2O/CH_3CN (1:1 v/v) mixture to circa 455 nm regardless of the supporting electrolyte used (see Fig. S8).

3.5. X-ray crystallography

A single crystal of $[Co(tpy)(phen)Cl](PF_6)_2$ was grown as an acetonitrile solvate by slow evaporation at first in acetonitrile solution; followed by the addition of acetone. The X-ray crystal structure for the dication of $[Co(tpy)(phen)Cl](PF_6)_2$ is shown in Fig. 3, with selected structure refinement parameters given in Table 1.

Selected bond lengths and angles are shown in Table 2. The structural analysis revealed a distorted octahedral arrangement about to the cobalt(III) metal centre. The tpy ligand is coordinated in a tridentate fashion and is meridionally arranged about the cobalt(III) core with resulting tpy and phen ligands lying in perpendicular coordination planes to each other, with the chloro ligand completing the octahedron. This coordination behaviour, bond lengths, and angles observed here are similar to the analogous $[Rh(tpy)(Z)Cl]^{2+}$ (where Z = bpy or phen) species [43]. In particular, the Co-N bond to the central nitrogen atom of the tpy ligand is the shortest of tpy, and all the tpy Co-N bonds are marginally shorter than those to phen ligand, which is consistent with what is observed in the Rh(III) complex. The N5-Co1-Cl1 bond angle is almost 180°, the bond length is normal for Co–Cl bonds [44]. The charge of $[Co(tpy)(phen)Cl]^{2+}$ is counterbalanced by two PF_6^- anions. In the extended structure, these anions, along with acetonitrile solvent molecules, occupy voids between $[Co(tpy)(phen)Cl]^{2+}$.

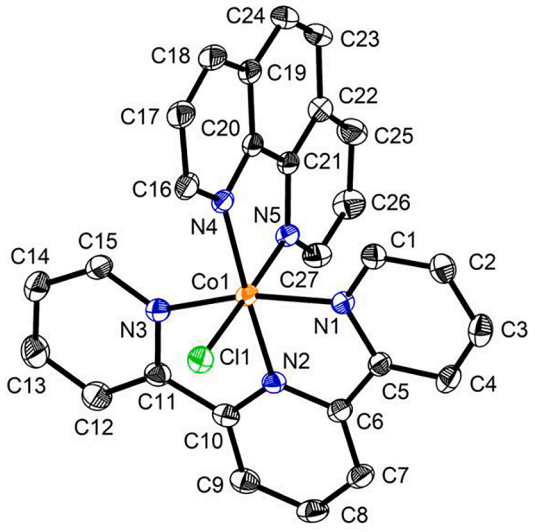

Fig. 3. Structure for the *mer*-$[Co(tpy)(phen)Cl]^{2+}$ complex as shown at 50% probability ellipsoids.

Table 1
Crystal data and structure refinement parameters for $[Co(tpy)(phen)Cl](PF_6)_2 \bullet 0.5CH_3CN$.

Identification code	$[Co(tpy)(phen)Cl](PF_6)_2$
Chemical formula	$C_{27}H_{19}ClCoF_{12}N_5P_2 \bullet 0.5C_2H_3N$
Formula weight (g/mol)	818.32
Crystal system, space group	monoclinic, C2/c
Unit cell dimensions (Å, °)	a = 30.0763(13)
	b = 14.5703(6)
	c = 14.9762(6)
	β = 114.3491(13)
Volume ($Å^3$)	5979.1(4)
Z, Calculated density (g cm^{-3})	8, 1.818
Reflections collected/unique	41055/6133
Data/restraints/parameters	6133/0/461
Final R indices [4838 data; I > 2σ(I)]	0.0348, 0.0722
R indices (all data)	0.0531, 0.0796
Largest diff. peak and hole	0.362, −0.421
CCDC no.	1953060

Table 2
Selected bond lengths and angles for $[Co(tpy)(phen)Cl](PF_6)_2 \bullet 0.5CH_3CN$.

Bond	Length (Å)	Bond	Length (Å)
Co1-N1	1.945(2)	Co1-N4	1.948(2)
Co1-N2	1.853(2)	Co1-N5	1.953(2)
Co1-N3	1.935(2)	Co1-Cl1	2.2241(8)
Bonds	Bond angle	Bonds	Bond angle
N2–Co1–N1	82.91(9)	N5–Co1–N4	85.04(9)
N2–Co1–N3	83.06(9)	N5–Co1–Cl1	177.80(7)
N1–Co1–N3	165.97(9)	N4–Co1–Cl1	93.86(7)
N2–Co1–N4	177.07(9)	N5–Co1–N3	91.11(9)
N2–Co1–Cl1	88.59(7)	N5–Co1–N1	90.00(9)
N2–Co1–N5	93.49(9)	N3–Co1–N4	98.54(9)
N1–Co1–N4	95.49(9)	N3–Co1–Cl1	89.86(7)
N1–Co1–Cl1	89.54(7)		

3.6. DFT and electrochemical studies

The complex, [Co(tpy)(phen)Cl]Cl, as reported by Chen et al. [11] showed remarkable activity in HER, especially when grafted (via electrochemical polymerization) on a Cu_2O surface. In their work, the $Co^{IV/III}$ and $Co^{III/II}$ couples showed reversible characteristics, however, the $Co^{II/I}$ redox couple showed little reversibility in acetonitrile. It was intriguing that the system was an efficient HER catalyst despite the apparent irreversibility of the $Co^{II/I}$ redox couple. It is therefore of interest to investigate the cyclic voltammetric characteristics of this species, bearing in mind the widely accepted view that a stable Co(I) species capable of undergoing reversible electron transfer is ideal for HER in cobalt-containing systems.

In the gas phase, DFT calculations at the EDF1/6-31G(d) level of theory predicted rings stretches and wagging of the polypyridyl rings at 1611, 1595, 1530, 1489, 1464, 1438 and 761 cm^{-1}, which are quite comparable to the observed values occurring at 1606, 1577, 1522, 1483, 1454, 1433, and 769 cm^{-1}, respectively. There is also a good comparison between the observed and calculated bond lengths and angles (see Table 3) where there calculated values differ from the observed values by less than 5%.

Analysis of the frontier molecular orbitals (Fig. 4) suggests that HOMO-1 through to the LUMO + 1 are all metal centered, and consequently, all the initial redox activities of $[Co(tpy)(phen)Cl]^{2+}$ are expected to be metal-based.

Cyclic and square wave voltammograms of $[Co(tpy)(phen)Cl](PF_6)_2$ in aqueous mixed solvents, and non-aqueous media revealed a series of (quasi-)reversible waves with $i_{pa}/i_{pc} = >0.9$ (Table 4). The peak potentials are scan rate dependent and showed negligible potential drift with increasing scan rate, consistent with their reversible nature. The $Co^{III/II}$ redox couple is observed between + 0.2 and + 0.4 V vs Ag/AgCl, whereas the $Co^{II/I}$ redox couple is observed between –0.8 and –0.9 V depending on the solvent and supporting electrolyte employed (see Fig. S9). In aqueous media, cobalt(II)-containing halides are well known to undergo rapid aquation [45], which can only be retarded by the presence of high halide concentration. In water, when NaCl was used as the supporting electrolyte it did not appear to improve the voltammetric reversibility of the electron transfers, and indeed a Co(I) species appears to be more unstable with NaCl compared to $NaClO_4$, resulting in a stripping wave on the return scan, due to the deposition of cobalt metal at the electrode surface (see Fig. S10). However, in the H_2O/CH_3CN (1:1, v/v) mixed solvent, improved voltammograms were obtained (see supporting information), and no stripping wave was observed. In the mixed solvent containing NaCl supporting electrolyte, the ΔE_p decreased to 80 mV which is closer to the 57 mV value expected for a one-electron Nernstian process, and was lower than that obtained with the $NaClO_4$ supporting electrolyte.

In CH_3CN, (Fig. 5 and Fig. S11), the voltammograms revealed reversible $Co^{III/II}$ and $Co^{II/I}$ redox couples which are slightly sensitive to the working electrode (by ca 60 mV between the GC and Pt electrodes), and are observed at $E_{½} = +0.29$ and –0.88 V vs Ag/AgCl, respectively, on a GC working electrode (WE). However, on reductively initiated scans on using Pt WE, a pre-wave is observed before the $Co^{II/I}$ redox couple. This pre-wave is present, albeit somewhat suppressed, on the GC WE and may be related to the enhanced lability of the chloride ligand in the + 2 oxidation state, which causes a subtle modification of the layer at the electrode surface. A third reversible wave at $E_{½} = –1.37$ V is most likely attributed to a one electron $Co^{I/0}$ redox couple, but may also involve one of the polypyridyl ligands as seen on the Pt WE. This is also suggested in the DFT calculations in which the LUMO + 1 is involves the tpy ligand system. On the return scan upon switching the potential at –2 V, the oxidation waves are slightly distorted and are likely related to the partial dissociation of the polypyridyl ligand(s) in the highly reduced state [41]. Additionally, as electrons are injected into the system, ΔE_p increased, indicating a drift from Nernstian behaviour. Nevertheless, the $Co^{II/I}$ redox couple showed reversible characteristics in all but the H_2O/NaCl combination.

The overall nature of the voltammogram in CH_3CN suggests that, on the electrochemical time scale, species with all three oxidation states of the cobalt metal centre, viz., +3, +2, and + 1, are fairly stable in nature, where $[Co(tpy)(phen)Cl](PF_6)_2$ may potentially be utilised as an electron shuttle in a reaction such as the hydrogen evolution reaction [11] amongst others. A plausible electron transfer mechanism is shown in Scheme 2.

Table 3
A comparison of selected bond lengths and angles determined from X-ray crystallography and those calculated by DFT methods EDF1/6-31G(d).

Bond	Length/Å		Bond	Length/Å	
	Observed	Calculated		Observed	Calculated
Co1-N1	1.945	1.959	Co1-N4	1.948	1.978
Co1-N2	1.853	1.859	Co1-N5	1.953	1.979
Co1-N3	1.935	1.959	Co1-Cl1	2.224	2.252
Bonds	Bond angle/°		Bonds	Bond angle/°	
	Observed	Calculated		Observed	Calculated
N2–Co1–N1	82.91(9)	82.55	N5–Co1–N4	85.04(9)	83.06
N2–Co1–N4	177.07(9)	179.61	N2–Co1–Cl1	88.59(7)	88.95

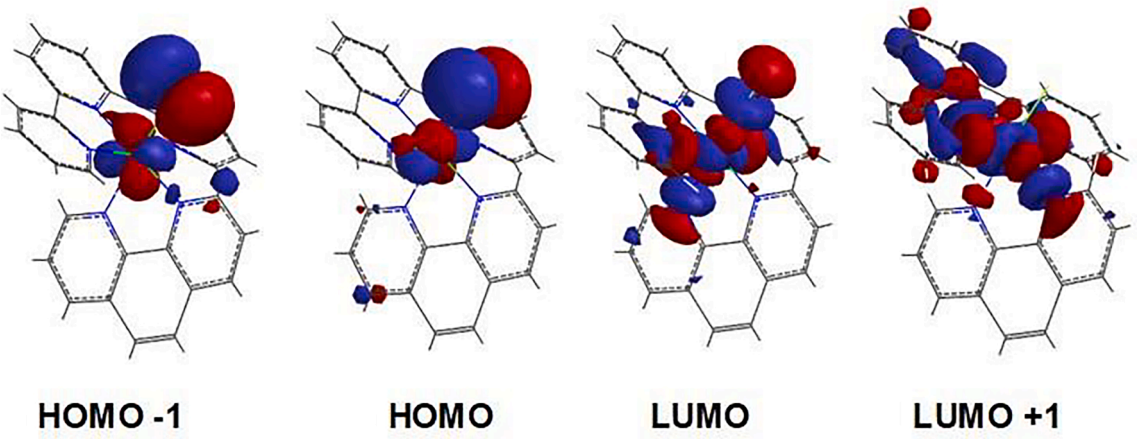

Fig. 4. Frontier molecular orbitals of $[Co(tpy)(phen)Cl]^{2+}$ calculated at the EDF1/6-31G(d) level of theory.

Table 4
Comparison of the reduction potentials of $[Co(tpy)(phen)Cl](PF_6)_2$ in H_2O and CH_3CN with various supporting electrolytes.

Redox couple	$E_{½}$/V	ΔE_p/mV	solvent	Electrolyte
$Co^{III/II}$	+0.22	320	H_2O	$NaClO_4$
	+0.23	–	H_2O	NaCl
	+0.32	109	H_2O/CH_3CN	$NaClO_4$
	+0.26	80	H_2O/CH_3CN	NaCl
	+0.29	126	CH_3CN	$[^nBu_4N]ClO_4$
	+0.35	92	CH_3CN	$[^nBu_4N]ClO_4$*
$Co^{II/I}$	−0.90	100	H_2O	$NaClO_4$
	−1.00	–	H_2O	NaCl
	−0.89	87	H_2O/CH_3CN	$NaClO_4$
	−0.88	83	H_2O/CH_3CN	NaCl
	−0.88	134	CH_3CN	$[^nBu_4N]ClO_4$
	−0.81	110	CH_3CN	$[^nBu_4N]ClO_4$*

* Pt working electrode

A series of spectroelectrochemical measurements were made on CH_3CN and H_2O/CH_3CN (1:1 v/v) mixed solvent solutions of $[Co(tpy)(phen)Cl](PF_6)_2$ (Fig. 6, S12 and S13). In the H_2O/CH_3CN (1:1 v/v) mixed solvent, Fig. S13, the $Co^{3+}\rightarrow Co^{2+}$ reduction resulted in a rapid increase in the absorbance at 460 nm along with a blue shift to 450 nm. This is succeeded by a gradual decrease in the absorbance across the spectrum. In the electrolysis of the solution at a potential sufficient to overcome the overpotential for the $Co^{2+}\rightarrow Co^{+}$ reduction, a similar pattern is observed at 460 nm, albeit a smaller change in the absorbance. A similar electrolysis in CH_3CN caused the peak that is observed circa 480 nm to first have a blue shift to circa 450 nm, followed by a decrease in the absorbance at this wavelength.

In addition to the blue shift in the d-d transitions, there is an increase in the absorbance across the UV region, suggestive of an increase in the charge transfer characteristics of the system associated with formation of a Co(I) species. The complex nature of the spectral transformation clearly indicates that the electrolysis did not have a simple A → B transformation. Here again, the exclusion of the chloride ligand from the coordination sphere maybe the cause of the biphasic nature of the spectral transformation. Electrolysis at –1.52 V (vs Ag/AgCl), also presented a biphasic spectrum, in which there is an initial rapid increase in the absorbance which is followed by decay towards a limiting value that is greater than the value prior to the electrolysis experiment. The transformation at this potential did not appear to share the blue shift observed at the more positive potential, and indeed is suggestive that the reduction may also involve the polypyridyl ligand(s).

3.7. Electrocatalytic studies

The effect of a proton source (*p*-cyanoanilinium tetrafluoroborate) on the voltammograms of $[Co(tpy)(phen)Cl](PF_6)_2$ in CH_3CN was investigated (Fig. 7). In the presence of *p*-cyanoanilinium tetrafluoroborate, a new cathodic wave is observed at ca –0.65 V of which the peak current increases with a simultaneous peak potential shift to increasingly negative values with increasing concentration of *p*-cyanoanilinium tetrafluoroborate. The adsorption pre-wave observed in the absence of the proton source is removed upon the addition of the *p*-cyanoanilinium tetrafluoroborate. The electrocatalytic wave was observed to occur initially ca 300 mV more positive than the $Co^{II/I}$ reduction wave, and displayed what is considered a "normal" catalysis [46–48], owing the lack of any apparent pre-wave or unexpected diffusional peaks. The production of hydrogen was confirmed from the analysis of the head space of a controlled potential electrolysis experiment involving the complex in the presence of *p*-cyanoanilinium tetrafluoroborate. In CH_3CN, the overpotential associated with the catalysed proton reduction was determined to be 830 mV. The magnitude of the Gibbs free energy for the homolytic and heterolytic hydrogen evolution from *p*-cyanoanilinium tetrafluoroborate in CH_3CN can be determined using the methodology suggested by Kellett and Spiro [49] on the basis

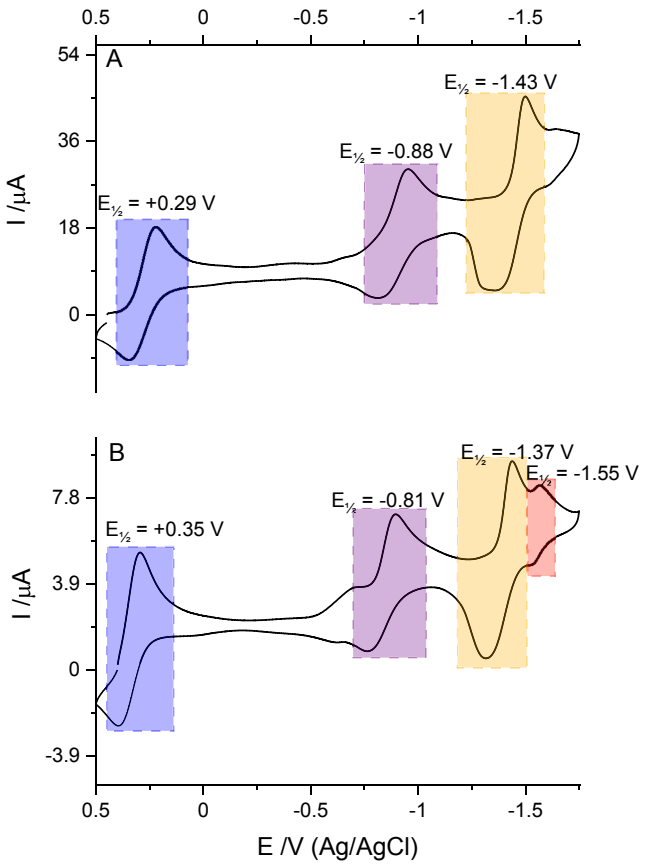

Fig. 5. Cyclic voltammogram of $[Co(tpy)(phen)Cl](PF_6)_2$. Solvent = acetonitrile, [complex] = 1.0 mM, $[^nBu_4N]ClO_4$ = 0.10 M, working electrode = (**A**) glassy carbon or (**B**) Pt, auxiliary electrode = Pt wire, reference electrode = Ag/AgCl, and scan rate = 100 mV s^{-1}.

$$[Co(tpy)(phen)Cl]^{2+} + e^- \leftrightarrow [Co(tpy)(phen)Cl]^+$$
$$[Co(tpy)(phen)Cl]^+ + e^- \leftrightarrow [Co(tpy)(phen)]^+ + Cl^-$$
$$[Co(tpy)(phen)]^+ + e^- \leftrightarrow [Co(tpy)(phen)]^0$$

Scheme 2. A plausible redox behaviour of $[Co(tpy)(phen)Cl](PF_6)_2$ in CH_3CN.

of the values for the potentials of the cobalt and HA/H_2 couples versus $Fc^{+/0}$. From the thermodynamic analysis of the heterolytic and the homolytic pathways, the free energies of ΔG = –15.4 and –56.9 kJ mol^{-1}, respectively, which suggests that the homolytic pathway is favoured thermodynamically.

3.8. Photocatalytic studies

Based on the electrochemical and spectroscopic results discussed above, the light driven hydrogen evolution reactions (HERs) for $[Co(tpy)(phen)Cl](PF_6)_2$ and the reference cobaloxime $[Co(dmgH)_2Cl(py)]$ were investigated, as polypyridyl and macrocyclic design for cobalt HER catalysts shows promising performances [39,50–55]. Unfortunately, the weak molar absorptivity of $[Co(tpy)(phen)Cl](PF_6)_2$ in the visible portion of the spectrum suggests that the complex is unlikely to be an intrinsic photosensitizer, and thus requires external activation. The most studied inorganic photosensitizer (PS), $[Ru(bpy)_3](PF_6)_2$ [39,52,56–58] was chosen to photo-reduce the Co HER catalysts. The samples were irradiated with blue LEDs centred at 445 nm, Fig. S14 and Table S2, in dimethylformamide as solvent, 1 M of triethanolamine as the sacrificial electron donor and 0.1 M aqueous tetrafluoroboric acid as the proton source, 0.1 mM of $[Ru(bpy)_3](PF_6)_2$, and the cobalt-containing catalysts

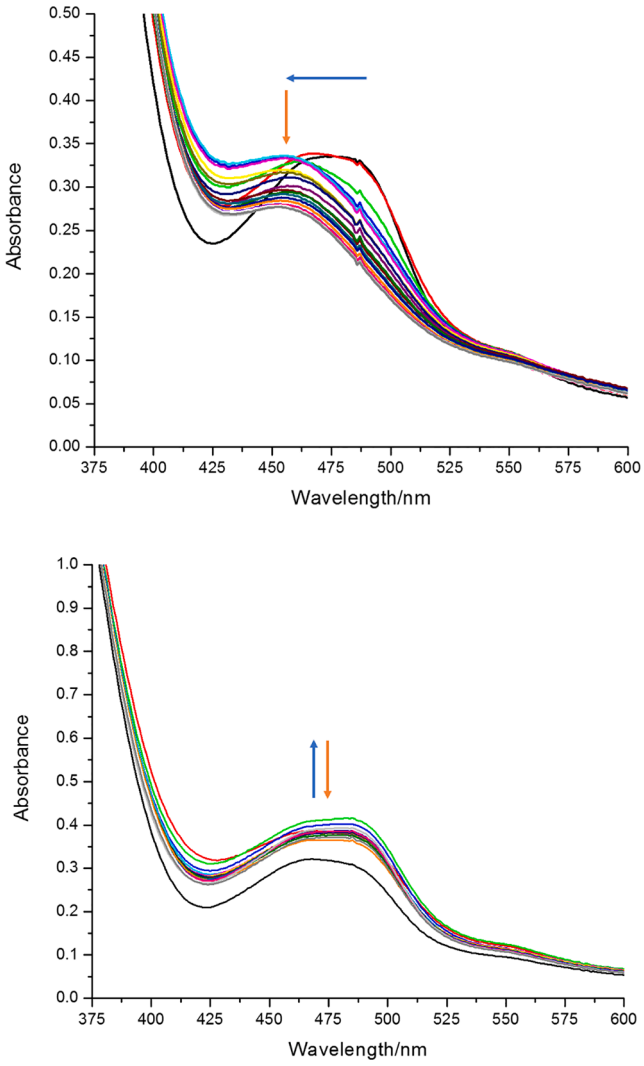

Fig. 6. Spectroelectrochemical transformations of $[Co(tpy)(phen)Cl](PF_6)_2$. Solvent = acetonitrile, [complex] = 14.9 mM, $[^nBu_4N]ClO_4$ = 0.10 M, working electrode = Pt mesh wire, auxiliary electrode = Pt wire, reference electrode = Ag/AgCl, held potential = –1.20 V (top) and –1.52 V (bottom), and path length = 1 mm.

at 0.01 mM. The $[Ru(bpy)_3](PF_6)_2$ is fully excited into the ^{1}MLCT band to drive the photoreactions. The excess of PS permits the evaluation of the maximum TON of HER cobalt-containing catalyst. No hydrogen was detected for the control experiments of the PS in the presence of sacrificial electron donor and HBF_4. When the illumination begins, a peak of activity occurred for both systems after a short lag time due to the required reduction of a Co(III) metal centre to a Co(I) metal centre [39]. The cobaloxime reaches a maximum turn over frequency (TOF) of 4500 $mmolH_2$ $mol^{-1}{}_{CAT}$ min^{-1} and $[Co(tpy)(phen)Cl](PF_6)_2$ attains 3300 mmol H_2 $mol^{-1}{}_{CAT}$ min^{-1} (Fig. 8). The activities decrease slowly to end after almost three hours. We observed a TON of 79 for $[Co(tpy)(phen)Cl](PF_6)_2$ and TON of 141 for the cobaloxime in ca 3 h of illumination. Aliquots of fresh photosensitizer and catalyst are added at the end of the photoreactions (Fig. S15). For both catalysts, the activity starts again with addition of photosensitizer and no revival is observed in the case of catalyst addition indicating that the photosensitizer decomposes first. These results are comparable to the other systems reported in a smorgasbord study of cobalt containing systems [30].

4. Conclusions

The X-ray crystallographic structure of $[Co(tpy)(phen)Cl](PF_6)_2$ is

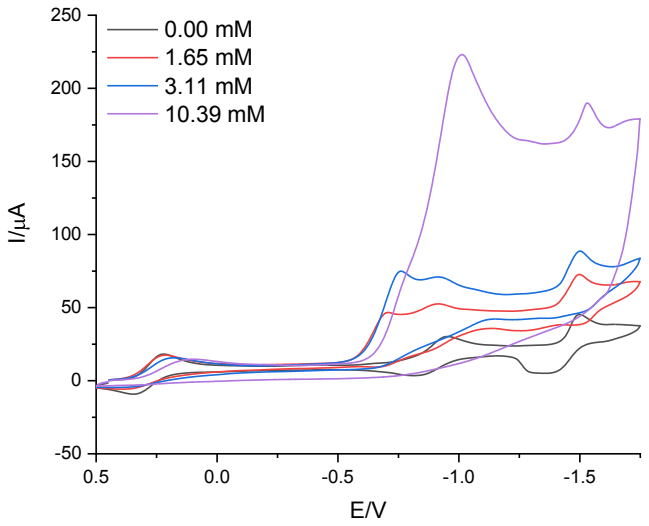

Fig. 7. Cyclic voltammograms illustrating the electrocatalytic behaviour of [Co(tpy)(phen)Cl](PF$_6$)$_2$. Solvent = acetonitrile, [complex] = 1.0 mM, [^{n}Bu$_4$N]ClO$_4$ = 0.10 M, working electrode = glassy carbon, auxiliary electrode = Pt wire, reference electrode = Ag/AgCl, and scan rate = 100 mV s^{-1}. The concentration of *p*-cyanoanilinium tetrafluoroborate was varied from 0.0 mM to 10 mM.

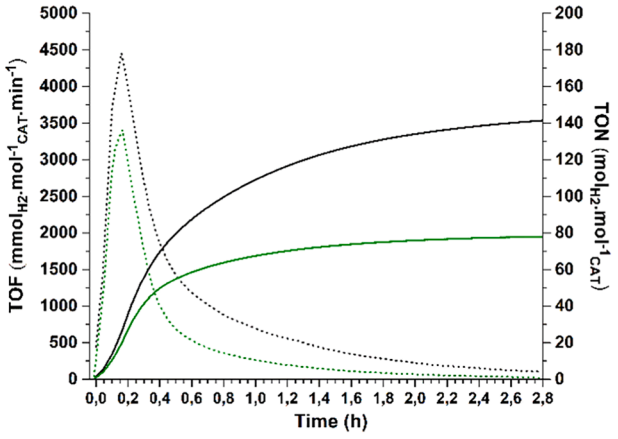

Fig. 8. Hydrogen evolution of [Co(dmgH)$_2$Cl(py)] (black) and [Co(tpy)(phen)Cl](PF$_6$)$_2$ (green). TOF: dotted line. TON: solid line. (For interpretation of the references to colour in this figure legend, the reader is referred to the web version of this article.)

presented, along with its spectroscopic and cyclic voltammetric properties. Unlike the report of its Co(II) analogue, we have demonstrated that that the Co(II/I) couple of [Co(tpy)(phen)Cl](PF$_6$)$_2$ possesses good reversible characteristics in aqueous and mixed aqueous environments. Like its analogous Co(II) counterpart, [Co(tpy)(phen)Cl](PF$_6$)$_2$ demonstrated excellent electrocatalytic hydrogen evolution at 830 mV overpotential in CH$_3$CN, as well as photocatalytic hydrogen evolution with a high turnover number and moderate turnover frequency in DMF over a 3 h period.

Declaration of Competing Interest

The authors declare that they have no known competing financial interests or personal relationships that could have appeared to influence the work reported in this paper.

Acknowledgements

AAH and MAWL would like to thank Professor Tara P. Dasgupta (sunrise: Wednesday, January 29, 1941 and sunset: Monday, April 20, 2020) for his beloved guidance as a father, a Ph.D. research advisor, and a mentor, to make us what we are today. R.I.P. AAH would also like to thank the National Science Foundation, 2415 Eisenhower Avenue, Alexandria, VA 22314, U.S.A., for a National Science Foundation CAREER Award, as this material is based upon work supported by the National Science Foundation under CHE-14321172 (formerly CHE-1151832). AAH would also like to thank the Old Dominion University startup package that allowed for the successful completion of this work. GSH, OS, and VP thank the Natural Sciences and Engineering Research Council (NSERC) of Canada (grant number 103046) for financial support.

Appendix A. Supplementary data

Supplementary data to this article can be found online at https://doi.org/10.1016/j.ica.2020.120195.

References

[1] N.S. Lewis, D.G. Nocera, Proc. Natl. Acad. Sci. U.S.A. 103 (2006) 15729.
[2] D.L. Royer, R.A. Berner, J. Park, Nature 446 (2007) 530.
[3] R.B. Gordon, M. Bertram, T.E. Graedel, Proc. Natl. Acad. Sci. U.S.A. 103 (2006) 1209.
[4] R.F. Service, Science 309 (2005) 548.
[5] D.Z. Zee, T. Chantarojsiri, J.R. Long, C.J. Chang, Acc. Chem. Res. 48 (2015) 2027–2036.
[6] V. Artero, M. Chavarot-Kerlidou, M. Fontecave, Angew. Chem. Int. Ed. 50 (2011) 7238–7266.
[7] T. Autrey, S. Xantheas, L. Li, J. Linehan, J. Franz, D. Katakis, C. Mitsopoulou, Z. Sofianos, T. Bitterwolf, Prepr. Pap. - Am. Chem. Soc., Div. Fuel Chem. 47 (2002) 752–754.
[8] M. Kobayashi, S. Masaoka, K. Sakai, Angew. Chem. Int. Ed. 51 (2012) 7431–7434.
[9] A.J. Esswein, D.G. Nocera, Chem. Rev. 107 (2007) 4022–4047.
[10] C.-B. Li, P. Gong, Y. Yang, H.-Y. Wang, Catal. Lett. 148 (2018) 3158–3164.
[11] X. Chen, H. Ren, W. Peng, H. Zhang, J. Lu, L. Zhuang, J. Phys. Chem. C 118 (2014) 20791–20798.
[12] M.A.W. Lawrence, M.J. Celestine, E.T. Artis, L.S. Joseph, D.L. Esquivel, A. J. Ledbetter, D.M. Cropek, W.L. Jarrett, C.A. Bayse, M.I. Brewer, A.A. Holder, Dalton Trans. 45 (2016) 10326–10342.
[13] G.A.N. Felton, R.S. Glass, D.L. Lichtenberger, D.H. Evans, Inorg. Chem. 45 (2006) 9181–9184.
[14] W. Gao, J. Ekström, J. Liu, C. Chen, L. Eriksson, L. Weng, B. Åkermark, L. Sun, Inorg. Chem. 46 (2007) 1981–1991.
[15] M.L. Helm, M.P. Stewart, R.M. Bullock, M.R. DuBois, D.L. DuBois, Science 333 (2011) 863–866.
[16] P.A. Jacques, V. Artero, J. Pecaut, M. Fontecave, Proc. Natl. Acad. Sci. U.S.A. 106 (2009) 20627–20632.
[17] O.R. Luca, S.J. Konezny, J.D. Blakemore, D.M. Colosi, S. Saha, G.W. Brudvig, V.S. Batista, R.H. Crabtree, New J. Chem. 36 (2012) 1149–1152.
[18] C. Baffert, V. Artero, M. Fontecave, Inorg. Chem. 46 (2007) 1817–1824.
[19] X. Hu, B.S. Brunschwig, J.C. Peters, J. Am. Chem. Soc. 129 (2007) 8988–8998.
[20] J. Wang, C. Li, Q. Zhou, W. Wang, Y. Hou, B. Zhang, X. Wang, Catal. Sci. Technol. 6 (2016) 8482–8489.
[21] P. Wang, G. Liang, C.L. Boyd, C.E. Webster, X. Zhao, Eur. J. Inorg. Chem. 2019 (2019) 2134–2139.
[22] P. Wang, G. Liang, M.R. Reddy, M. Long, K. Driskill, C. Lyons, B. Donnadieu, J. C. Bollinger, C.E. Webster, X. Zhao, J. Am. Chem. Soc. 140 (2018) 9219–9229.
[23] M.A.W. Lawrence, A.A. Holder, Inorg. Chim. Acta 441 (2016) 157–168.
[24] P. Du, J. Schneider, G. Luo, W.W. Brennessel, R. Eisenberg, Inorg. Chem. 48 (2009) 4952–4962.
[25] W.T. Eckenhoff, R. Eisenberg, Dalton Trans. 41 (2012) 13004–13021.
[26] S. Varma, C.E. Castillo, T. Stoll, J. Fortage, A.G. Blackman, F. Molton, A. Deronzier, M.N. Collomb, Phys. Chem. Chem. Phys. 15 (2013) 17544–17552.
[27] M.G. Pfeffer, B. Schäfer, G. Smolentsev, J. Uhlig, E. Nazarenko, J. Guthmuller, C. Kuhnt, M. Wächtler, B. Dietzek, V. Sundström, S. Rau, Angew. Chem. Int. Ed. 54 (2015) 5044–5048.
[28] S. Shi, L.M. Daniels, J.H. Espenson, Inorg. Chem. 30 (1991) 3407–3410.
[29] O.M. Williams, A.H. Cowley, M.J. Rose, Dalton Trans. 44 (2015) 13017–13029.
[30] R.W. Hogue, O. Schott, G.S. Hanan, S. Brooker, Chem. - Eur. J. 24 (2018) 9820–9832.
[31] T. Taura, Bull. Chem. Soc. Jpn. 63 (1990) 1105–1110.
[32] M.S. Gordon, M.W. Schmidt, Chapter 41 - Advances in electronic structure theory: GAMESS a decade later, in: C.E. Dykstra, G. Frenking, K.S. Kim, G.E. Scuseria (Eds.) Theory and Applications of Computational Chemistry, Elsevier, Amsterdam, 2005, pp. 1167–1189.

[33] M.W. Schmidt, K.K. Baldridge, J.A. Boatz, S.T. Elbert, M.S. Gordon, J.H. Jensen, S. Koseki, N. Matsunaga, K.A. Nguyen, S. Su, T.L. Windus, M. Dupuis, J. A. Montgomery Jr, J. Comput. Chem. 14 (1993) 1347–1363.
[34] V.A. Rassolov, J.A. Pople, M.A. Ratner, T.L. Windus, J. Chem. Phys. 109 (1998) 1223–1229.
[35] V.A. Rassolov, M.A. Ratner, J.A. Pople, P.C. Redfern, L.A. Curtiss, J. Comput. Chem. 22 (2001) 976–984.
[36] R.D. Adamson, P.M.W. Gill, J.A. Pople, Chem. Phys. Lett. 284 (1998) 6–11.
[37] B.M. Bode, M.S. Gordon, J. Mol. Graphics Model. 16 (1999) 133–138.
[38] G.M. Sheldrick, SHELXL 2014/7, University of Gottngen, Germany, 2014.
[39] O. Schott, A.K. Pal, D. Chartrand, G.S. Hanan, Chemsuschem 10 (2017) 4436–4441.
[40] B. Brisig, E.C. Constable, C.E. Housecroft, New J. Chem. 31 (2007) 1437–1447.
[41] M.A.W. Lawrence, C.D. McMillen, R.K. Gurung, M.J. Celestine, J.F. Arca, A. A. Holder, J. Chem. Crystallogr. 45 (2015) 427–433.
[42] A. Yamasaki, F. Yajima, S. Fujiwara, Inorg. Chim. Acta 2 (1968) 39–42.
[43] M.Y. Kim, W.K. Seok, Y. Dong, H. Yun, Inorg. Chim. Acta 319 (2001) 194–198.
[44] D.A. House, Comments Inorg. Chem. 19 (1997) 327–350.
[45] F.P. Rotzinger, Inorg. Chem. 38 (1999) 5730–5733.
[46] K.J. Lee, B.D. McCarthy, J.L. Dempsey, Chem. Soc. Rev. 48 (2019) 2927–2945.
[47] C. Costentin, J.-M. Savéant, ChemElectroChem 1 (2014) 1226–1236.
[48] C. Costentin, H. Dridi, J.-M. Savéant, J. Am. Chem. Soc. 136 (2014) 13727–13734.
[49] R.M. Kellett, T.G. Spiro, Inorg. Chem. 24 (1985) 2373–2377.
[50] N. Queyriaux, R.T. Jane, J. Massin, V. Artero, M. Chavarot-Kerlidou, Coord. Chem. Rev. 304–305 (2015) 3–19.
[51] S. Rajak, O. Schott, P. Kaur, T. Maris, G.S. Hanan, A. Duong, RSC Adv. 9 (2019) 28153–28164.
[52] R.W. Hogue, O. Schott, G.S. Hanan, S. Brooker, Chemistry 24 (2018) 9820–9832.
[53] R.S. Khnayzer, V.S. Thoi, M. Nippe, A.E. King, J.W. Jurss, K.A. El Roz, J.R. Long, C. J. Chang, F.N. Castellano, Energ. Environ. Sci. 7 (2014) 1477–1488.
[54] D.Z. Zee, T. Chantarojsiri, J.R. Long, C.J. Chang, Acc. Chem. Res. 48 (2015) 2027–2036.
[55] W.K. Lo, C.E. Castillo, R. Gueret, J. Fortage, M. Rebarz, M. Sliwa, F. Thomas, C. J. McAdam, G.B. Jameson, D.A. McMorran, J.D. Crowley, M.N. Collomb, A. G. Blackman, Inorg. Chem. 55 (2016) 4564–4581.
[56] P. Dongare, B.D.B. Myron, L. Wang, D.W. Thompson, T.J. Meyer, Coord. Chem. Rev. 345 (2017) 86–107.
[57] E. Rousset, D. Chartrand, I. Ciofini, V. Marvaud, G.S. Hanan, Chem. Commun. (Camb.) 51 (2015) 9261–9264.
[58] E. Rousset, I. Ciofini, V. Marvaud, G.S. Hanan, Inorg. Chem. 56 (2017) 9515–9524.